High-Resolution ^{113}Cd NMR of Solids. Correlation of Spectra with the Molecular Structure of a Decanuclear Cadmium(II) Complex

P. DuBois Murphy, W. C. Stevens, T. T. P. Cheung, S. Lacelle, B. C. Gerstein,* and D. M. Kurtz, Jr.*

Contribution from the Ames Laboratory, Department of Energy and Department of Chemistry, Iowa State University, Ames, Iowa 50011. *Received December 1, 1980*

Abstract: The usefulness of ^{113}Cd NMR in solution as a structural and dynamic probe of macromolecular systems is hampered by fast exchange of Cd^{2+} with ligands and solvent. This paper demonstrates that recently developed techniques for attainment of high-resolution NMR spectra in solids can overcome this problem. These spectra provide information about Cd^{2+} coordination environments which is unavailable in solution and which can be used to interpret NMR spectra in solution. By a combination of ^{113}Cd-^{1}H cross polarization and spinning either at the magic angle or slightly off magic angle, the following solid-state ^{113}Cd NMR data for each cadmium site in the decanuclear cation $Cd_{10}(SCH_2CH_2OH)_{16}^{4+}$ have been obtained: $\bar{\sigma}$, the isotropic value of the chemical shift; $\Delta\sigma$, the shielding anisotropy; and S, a symmetry factor which characterizes the uniformity of shielding with respect to an axially symmetric tensor. The values of $\bar{\sigma}$ and $\Delta\sigma$ are shown to accurately reproduce the static (nonspinning) NMR spectrum of the solid. The NMR results are correlated with the known structure of this ion. We conclude that (1) $\bar{\sigma}$ indicates the kinds of nearest neighbors much as does a solution NMR spectrum but without the complication of chemical exchange; (2) the shielding anisotropies, $\Delta\sigma$, indicate the range of bonding distances of nearest neighbors; (3) a high value of the symmetry factor S indicates axial or near-axial shielding symmetry but does not necessarily imply a low value of $\Delta\sigma$. The values of S reflect approximate local site symmetries. Our chemical shift data for the decanuclear cation in the solid state agree quite well with the published solution spectra, and from these data an estimate is made of the exchange rate between CdS_4 and CdS_4O sites of this ion in solution. All of the spectra were obtained on samples unenriched beyond the natural isotopic abundance of ^{113}Cd (12.34%). Our data suggest that the ^{113}Cd resonances observed for metallothionen are due to CdS_4 coordination sites and not to CdS_4O or CdS_3O_3 sites.

Introduction

The usefulness of the ^{113}Cd nucleus ($I = {}^1/_2$, 12.3% natural isotopic abundance, 1.09×10^{-2} sensitivity at constant field compared with an equal number of protons) as a probe of the static and dynamic coordination environment of Cd^{2+} in both inorganic complexes and in metalloproteins is well documented by NMR studies in solution.[1-5] The observed chemical shift dispersion of over 800 ppm implies that the shielding of the ^{113}Cd nucleus is extremely sensitive to its local environment. However, attempts to make detailed correlations of solution NMR spectra with coordination environments in cadmium compounds of known structure are hampered by concentration and temperature-dependent chemical shifts due to exchange with ligands and solvent at rates which are fast on the NMR time scale.[2,5]

Recently developed techniques for attainment of high-resolution NMR spectra in the solid state[5-9] could theoretically remove this difficulty since for solids one expects chemical exchange to be extremely slow or absent. Also, one can obtain NMR spectra of solids such that chemical shifts either are or are not averaged to their isotropic values. The chemical shift anisotropy reflects the site symmetry of a nucleus but this information is lost in solution. Therefore, high-resolution ^{113}Cd NMR spectroscopy of solids presents the possibilities of (1) correlating coordination environments of Cd^{2+} with isotropic chemical shifts in the absence of chemical exchange and (2) correlating crystallographically determined site symmetries with chemical shift anisotropies. Such correlations could then be applied to ^{113}Cd NMR spectra of materials such as Cd^{2+} containing proteins in both solution and solid states.

One of the first successful attempts to obtain high-resolution NMR spectra of metals in the solid state was that of Andrew et al.[10] who were able to remove much of the broadening due to chemical shift anisotropy of ^{113}Cd in metallic cadmium. Since that time we and others[5,9,11] have found that the combined techniques of ^{113}Cd-^{1}H cross polarization (CP), which enhances signal and removes broadening due to heteronuclear dipolar coupling,[6,7] and magic angle spinning (MAS), which removes broadening due to chemical shift anisotropy,[12] can be successfully applied to simple inorganic salts of cadmium in the solid state without enriching beyond the natural isotopic abundance of ^{113}Cd.

We report here the results of our first attempt to make the molecular structural correlations referred to above on other simple cadmium salts. We chose the decanuclear cation $Cd_{10}(SCH_2CH_2OH)_{16}^{4+}$ because its molecular structure is known (Figure 1),[13,14] its ^{113}Cd NMR spectra in solution have been studied,[1] and its coordination environments may model those of Cd^{2+} in some proteins, particularly metallothionen.[4]

Experimental Section

Instrumental Data. Excitations of ^{113}Cd and ^{1}H cross polarization (CP) were at 12.42 and 56.02 MHz, respectively, in our 1.3-T laboratory field. The design of the CP spectrometer has been described in detail elsewhere.[9] Rotating-frame H_1 fields of 8 and 36.1 G matched the

(1) Cardin, A. D.; Ellis, P. D.; Oden, J. D.; Howard, J. W. *J. Am. Chem. Soc.* **1975**, *97*, 1672-1679.
(2) Haberkorn, R. A.; Que, L., Jr.; Gillum, W. O.; Holm, R. H.; Liu, E. S.; Lord, R. C. *Inorg. Chem.* **1976**, *15*, 2408-2414.
(3) Armitage, I. M.; Schoot-Uiterkamp, A. J. M.; Chlebowski, J. F.; Coleman, J. E. *J. Magn. Reson.* **1978**, *29*, 375-392.
(4) (a) Otvos, J. D.; Armitage, I. M. *J. Am. Chem. Soc.* **1979**, 101, 7734-36. (b) *Proc. Natl. Acad. Sci.U.S.A.* **1980**, *77*, 7094-7098.
(5) Ackerman, J. J. H.; Orr, T. V.; Bartuska, V. J.; Maciel, G. E. *J. Am. Chem. Soc.* **1979**, *101*, 341-347.
(6) Pines, A.; Gibby, M. G.; Waugh, J. G. *J. Chem. Phys.* **1973**, *59*, 569-590.
(7) Mehring, M. "High Resolution NMR Spectroscopy in Solids", Springer-Verlag, Berlin, 1976.
(8) Taylor, R. E.; Pembleton, R. G.; Ryan, L. M.; Gerstein, B. C. *J. Chem. Phys.* **1979**, *71*, 4541-4545.
(9) Cheung, T. T. P.; Worthington, L.; Murphy, P. DuBois; Gerstein, B. C. *J. Magn. Reson.* **1980**, *41*, 158-168.
(10) Andrew, E. R.; Hinshaw, W. S.; Tiffen, R. S. *J. Magn. Reson.* **1974**, *15*, 191-194.
(11) Murphy, P. DuBois; Gerstein, B. C. *J. Am. Chem. Soc.*, in press.
(12) Andrew, E. R.; Eades, R. G. *Discuss. Faraday Soc.* **1962**, *34*, 38-42.
(13) Strickler, P. *Chem. Commun.* **1969**, 655-656.
(14) Schwarzenbach, G.; Gaulschi, K.; Peter, J.; Tunaboyler, K. *Trans. R. Inst. Technol. Stockholm* **1972**, No. 271, 295-304.

0002-7863/81/1503-4400$01.25/0

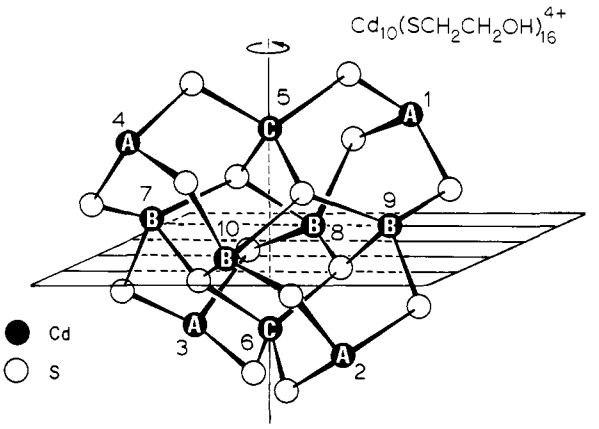

Figure 1. The Cd–S framework of $Cd_{10}(SCH_2CH_2OH)_{16}^{4+}$. The lettering indicates CdS_3O_3 (A), CdS_4O (B), and CdS_4 (C) coordination environments and also refers to the assignments of resonances in Figure 2. Detailed depictions of each coordination environment can be found in ref 13 and 14.

Hartmann–Hahn condition at the magic angle (54.7°).[15] Magic angle spinning (MAS) measurements were made on about 0.3 g of powdered samples with a rotor speed of 2.9 kHz. Data were acquired with coherent signal-averaging of 15 000 scans with periods between accumulations of 3 s. The magic angle (54.7°) was determined by calibration for minimum line width on a cadmium nitrate tetrahydrate standard. The residual line width at the magic angle was 1.5 ppm (parts per million) for $Cd(NO_3)_2{\cdot}4H_2O$ and is mainly limited by dc magnetic inhomogeneity as well as slight offsets from the magic angle. CP contact times were 4 ms. Static spectra of $[Cd_{10}(SCH_2CH_2OH)_{16}](ClO_4)_4$ were recorded with a spectrometer offset of 5 kHz below the $\sigma_\perp$ of the A band and with a low-frequency amplifier bandwidth of 33 kHz; MAS and OMAS (off-magic angle spinning) spectra were recorded with the same offset but with a 20-kHz bandwidth. Spectra of $Cd(ClO_4)_2$ in aqueous solution were obtained at 25 °C in 10-mm tubes by conventional single pulse methods (no CP or MAS).

All spectra were corrected for (1) frequency rolloff from the low-pass filter of the low-frequency amplifier and (2) linear phase errors which result from time delays in the digitalization of the free induction decays. Chemical shift scales were calibrated with respect to the isotropic line of an external reference of $Cd(NO_3)_2{\cdot}4H_2O$ recorded under identical MAS conditions (exchange method). Corrections for bulk susceptibilities were not made. In accordance with the accepted σ convention used in solid-state NMR,[7-11,16] negative shifts are downfield from the reference and indicate decreased shieldings.

Preparation and Characterization of Samples. $Cd(NO_3)_2{\cdot}4H_2O$, $Cd(ClO_4)_2{\cdot}6H_2O$, CdO, and CdS (Alpha ultrapure grade) were obtained commercially and used without further purification. $[Cd_{10}(SCH_2CH_2OH)_{16}](ClO_4)_4$ was prepared according to the method of Schwarzenbach et al.[14] Analysis of this compound by Galbraith Laboratories, Inc., was consistent with the anhydrous formulation of Haberkorn et al.[2] Anal. Calcd for $C_{32}H_{80}Cd_{10}Cl_4O_{32}S_{16}$: C, 13.95; H, 2.93; Cd, 40.79; Cl, 5.15; S, 18.62. Found: C, 14.18; H, 3.07; Cd, 40.88; Cl, 5.02; S, 18.35. All of the samples used in this study contained the natural isotopic abundance (12.34%) of ^{113}Cd.

The unit cell parameters of $[Cd_{10}(SCH_2CH_2OH)_{16}](ClO_4)_4$ were determined from rotation photographs obtained on a Syntex four-circle X-ray diffractometer and verified from oscillation photographs obtained on a home-built diffractometer in the Ames Laboratory.

Theory and Experimental Guidelines

Because this paper describes the first application of ^{113}Cd–^1H CP, MAS, and OMAS to other than simple cadmium salts, we wish to establish what we believe should be some theoretical and experimental guidelines for obtaining and analyzing such data.

Theory. The three principal components of the chemical shift shielding tensor σ_{11}, σ_{22}, and σ_{33} are directly measureable from NMR spectra of powdered samples provided that the problem of overlapping tensors can be appropriately handled.[8,9,11] The tensors are observed experimentally as "powder patterns".

One can usefully characterize and compare the shieldings of different species with three general quantities derived from the principal components: $\bar{\sigma}$, the isotopic or average value of the shielding; $\Delta\sigma$, a number characterizing the shielding anisotropy; and S, a symmetry factor.

For a nonaxially symmetric tensor, the quantities $\bar{\sigma}$, $\Delta\sigma$, and S are defined:

$$\bar{\sigma} = (\sigma_{11} + \sigma_{22} + \sigma_{33})/3 \quad (1)$$

For $(\sigma_{22} - \sigma_{11}) < (\sigma_{33} - \sigma_{22})$:

$$\Delta\sigma = \sigma_{33} - \tfrac{1}{2}(\sigma_{11} + \sigma_{22}) \quad (2)^{16}$$

$$S = 1 - (\sigma_{22} - \sigma_{11})/(\sigma_{33} - \sigma_{22}) \quad (3)$$

For $(\sigma_{33} - \sigma_{22}) < (\sigma_{22} - \sigma_{11})$:

$$\Delta\sigma = \sigma_{11} - \tfrac{1}{2}(\sigma_{22} + \sigma_{33}) \quad (4)$$

$$S = 1 - (\sigma_{33} - \sigma_{22})/(\sigma_{22} - \sigma_{11}) \quad (5)$$

For an axially symmetric tensor, two cases are possible:

$$(\sigma_{11} = \sigma_{22} = \sigma_\perp) < (\sigma_{33} = \sigma_\parallel) \quad (6)$$

and

$$(\sigma_{11} = \sigma_\parallel) < (\sigma_{22} = \sigma_{33} = \sigma_\perp) \quad (7)$$

Substituting these relationships into eq 1–5 yields

$$\bar{\sigma} = (2\sigma_\perp + \sigma_\parallel)/3 \quad (8)$$

$$\Delta\sigma = \sigma_\parallel - \sigma_\perp \quad (9)$$

$$S = 1 \quad (10)$$

For an axially symmetric tensor, both eq 2 and 4 reduce to eq 9 and both eq 3 and 5 reduce to eq 10.

For an isotropic tensor, all three components are equal

$$\sigma_{11} = \sigma_{22} = \sigma_{33} = \sigma_{iso} \quad (11)$$

with the result

$$\bar{\sigma} = \sigma_{iso} \quad (12)$$

$$\Delta\sigma = 0 \quad (13)$$

$$S(\text{indeterminate}) \quad (14)$$

The symmetry factor S ranges in value from 0 to 1 for a nonaxially symmetric tensor; however, S is always unity for an axially symmetric tensor, because only two values (i.e., $\bar{\sigma}$ and $\Delta\sigma$) are required to fully describe this shielding. While isotropic values, $\bar{\sigma}$, characterize the average relative shielding of different species, anisotropies, $\Delta\sigma$, and symmetry factors, S, are more characteristic of the local, three-dimensional shielding environment of a given species.

To achieve the rapid rotation limit[8] in both CP MAS and CP OMAS spectra, the inequality

$$\omega_r > R \quad (15)$$

$$R = \omega_0|\sigma_i - \bar{\sigma}| \quad (16)$$

must be satisfied where ω_r is the rotational frequency, ω_0 is the Larmor frequency, and σ_i is one of the three tensor components chosen such that $|\sigma_i - \bar{\sigma}|$ is maximum. Failure to satisfy the inequality (15) results in the appearance of spinning satellites whose amplitudes correlate with the magnitude of the violation of the inequality.[17]

The OMAS technique,[8,11] is used to resolve and measure the components of the shielding tensors of overlapping resonances. OMAS spectra are obtained by setting the sample rotation axis off of the magic angle (54.7°) by a value typically less than ±5°. A proper choice of the inclination angle, θ, results in a spectrum containing scaled but nonoverlapping powder patterns of shielding tensors. The observed OMAS shielding components, σ_i', are scaled with respect to their isotropic value by a constant C which depends

(15) Hartmann, S. R.; Hahn, E. L. *Phys. Rev.* **1962**, *128*, 2042–2053.
(16) Wemmer, D. E.; Pines, A. *J. Am. Chem. Soc.* **1981**, *103*, 34–36.
(17) Herzfeld, J.; Berger, A. E. *J. Chem. Phys.* **1980**, *73*, 6021–6030.

Table I. ^{113}Cd NMR Spectral Parameters for $[Cd_{10}(SCH_2CH_2OH)_{16}](ClO_4)_4$

^{113}Cd type	shielding symmetry[a]	$\sigma_{11}/\sigma_{\parallel}$,[b] ±5 ppm	$\sigma_{22}/\sigma_{\perp}$,[b] ±5 ppm	σ_{33},[b] ±5 ppm	$\bar{\sigma}$,[c] ±5 ppm	$\Delta\sigma$,[c] ±10 ppm	S,[c] ±0.05	FWBF,[d] ±5 ppm	R,[e] ±50 Hz	% area static, ±3%	$\bar{\sigma}_{MAS}$,[f] ±5 ppm	% area MAS, ±3%	FWHM,[g] ±0.5 ppm
A	AS	−706	−411		−509	−295	1.0	33	2448	43	−509	43	6.4
B	NS	−990	−480	−337	−603	−582	0.72	15	4808	38	−602	38	5.6
C	NS	−902	−779	−642	−774	199	0.10	14	1702	19	−773	19	7.2

[a] AS = axially symmetric; NS = nonaxially symmetric. [b] Tensor components determined by least-squares analysis;[21] shifts in ppm, with respect to $Cd(NO_3)_2 \cdot 4H_2O$; more negative shifts indicate decreased shielding. The tabulation follows the accepted σ convention: $\sigma_{11} \leq \sigma_{22} \leq \sigma_{33}$. [c] These generalized parameters are calculated with eq 1-10. [d] Full width at half-maximum of Gaussian broadening function used to fit residual broadening. [e] R is calculated with eq 16. [f] First moments in ppm. [g] Full width at half-maximum approximated as $2\sqrt{2 \ln 2}$ times the square root of the second moment.

Table II. OMAS ^{113}Cd NMR Spectral Parameters for $[Cd_{10}(SCH_2CH_2OH)_{16}](ClO_4)_4$

θ, ±0.1	^{113}Cd type	shielding[a] symmetry	$\bar{\sigma}$,[b,c] ±5 ppm	$\Delta\sigma'$,[c] ±5 ppm	S,[c] ±0.1	FWBF,[d] ±1 ppm	% area,[e] ±3%	calcd[f] $\Delta\sigma$ ±10 ppm
51.0	A	AS	−510	−25.5	1.0	5.7	46	−271
	B	NS	−603	−53.5	0.73	6.6	32	−569
	C	NS	−771	19.6	0.14	4.6	22	208
60.4	A	AS	−511	38.3	1.0	6.2	48	−286
	B	NS	−600	77.6	0.77	7.0	34	−579
	C	NS	−772	−26.5	0.0	6.7	19	198

[a-d] Same as for Table I. [e] Not corrected for area of spinning sidebands. [f] $C = (3\cos^2\theta - 1)/2$; $\Delta\sigma_{AS} = \Delta\sigma_{AS}'/C$; $\Delta\sigma_{NS} = \Delta\sigma_{NS}'/C$.

on the inclination angle, θ. The actual static (nonspinning) tensor components, σ_i, can be calculated from the OMAS scaled components, σ_i', by the following relations:

$$\sigma_i = (\sigma_i' - \bar{\sigma})/C + \bar{\sigma} \quad (17)$$

$$C = (3\cos^2\theta - 1)/2 \quad (18)$$

The values of the scaled shielding components are measured by nonlinear least-squares analyses.

Experimental Guidelines. The inferred static shielding components, σ_i, which are derived from the scaled OMAS shielding components, σ_i', using equations 17 and 18 may have relatively large experimental uncertainties (±20% is not uncommon) primarily because of errors in two procedures: (1) extraction of the scaled shielding components by nonlinear least-squares analysis and (2) determination of the rotational angle, θ. In general, the extraction of shielding components becomes more reliable as the separations between these components increase; however, maximum offsets from the magic angle may have to kept small if the problem of overlapping powder patterns of tensors is to be avoided. The second problem is by far the more serious since small errors in θ (which is usually within 5°, or so, of the magic angle) can lead to enormous uncertainties in the inferred static values of the shielding components (eq 17 and 18). For instance, in our laboratory, the magic angle can be reproducibly set to within ±0.1°; however, offsets from this angle are generally measurable to no better than ±0.5°.

One way to minimize this problem is to check for consistency of the inferred static values from determinations at both positive and negative offsets from the magic angle. Note that the scaled tensors obtained from spectra at equal positive and negative offsets should be mirror images of each other. However, the most powerful means to ensure accuracy, we believe, is the synthesis of the static spectrum. While OMAS-measured shielding components may have relatively high uncertainties, these values are sufficiently accurate to serve as "initial guesses" in the synthesis of the static spectrum. The values of the shielding components and other parameters, such as the widths of the broadening functions, are optimized until the residual (sum of errors)^2 changes by less than 0.01 for two consecutive iterations of the parameters.

There are two spectral measurements that certainly must be consistent within experimental precision for the static and MAS spectra which are recorded under the same CP contact time. First, the isotropic values of the shielding tensors, eq 1, 8, and 11, and the first moments (i.e., "centers of gravity") of the MAS absorptions should be equivalent. Second, the relative areas bounded

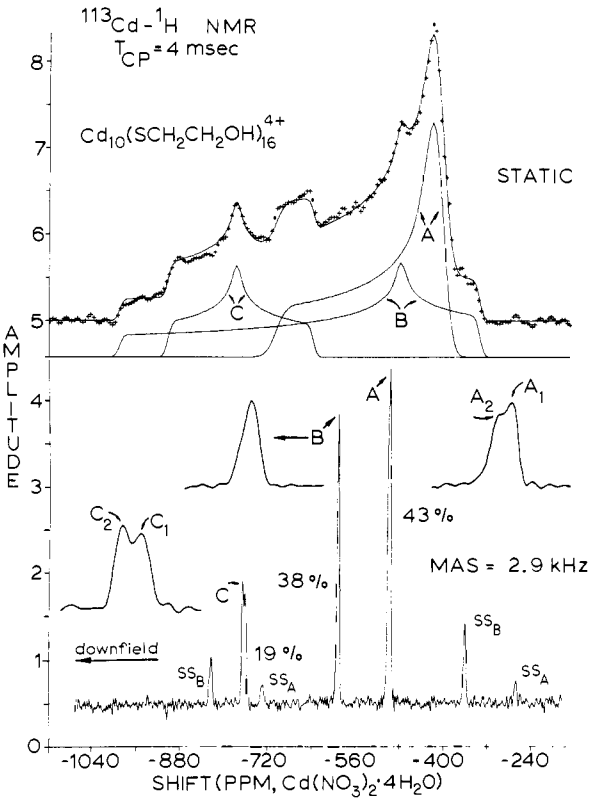

Figure 2. ^{113}Cd-^{1}H CP NMR spectra of powdered $[Cd_{10}(SCH_2CH_2OH)_{16}](ClO_4)_4$. (Top) Static spectrum. "+" indicates actual data point; solid lines indicate the fitted powder patterns of shielding tensors for each resonance A, B, and C and their addition to fit the observed spectrum. (Bottom) MAS spectrum. Insets show resolution of resonances A, B, and C. Spectral conditions not given in the figure appear in the Experimental Section.

by the powder patterns of the shielding tensors should agree with the same relative areas observed in the MAS spectrum. We believe synthesis of the static spectrum and coincidence of the above conditions are absolutely essential for maximum accuracy in determination of the shielding tensor along the principal axes, particularly in complicated systems such as the ^{113}Cd NMR of $Cd_{10}(SCH_2CH_2OH)_{16}^{4+}$. Furthermore, because of the high possibilities of erroneous measurements from the use of the OMAS alone, we feel that synthesis of the static spectrum is absolutely

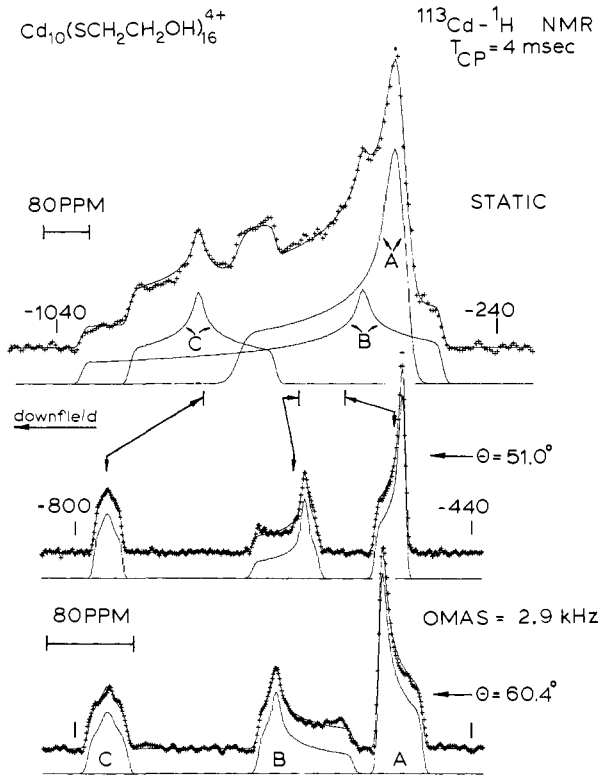

Figure 3. Comparison of static and OMAS spectra of $[Cd_{10}(SCH_2CH_2OH)_{16}](ClO_4)_4$. The top spectrum is identical with the top spectrum in Figure 2. The vertical lines below the top spectrum indicate isotropic values of the chemical shifts, $\bar{\sigma}$. The middle and bottom spectra were recorded at the indicated inclination angles, θ. Other conditions were the same as in Figure 2.

necessary to confirm the OMAS assignments.

Results

The static (nonspinning) and high-resolution MAS solid-state ^{113}Cd spectra of powdered $[Cd_{10}(SCH_2CH_2OH)_{16}](ClO_4)_4$ are shown in Figure 2, and appropriate spectral information is tabulated in Table I. The OMAS ^{113}Cd spectra recorded for both positive and negative offsets from the magic angle are shown in Figure 3, and appropriate spectral information is tabulated in Table II.

The MAS spectrum shows three major resonances labeled A, B, and C. Therefore, there are at least three types of magnetically inequivalent Cd^{2+} sites in the decanuclear cation. We shall refer to these sites as Cd(A), Cd(B) and Cd(C), respectively. The minor absorption peaks are spinning satellites (sidebands). We have labeled these SS_A and SS_B and subscripts refer to the parent absorption. Measurements of the MAS spectrum at different rotor speeds confirm the identity of these spinning satellites. The area ratios, including contributions from sidebands, are found to be A:B:C = 4.3: 3.8:1.9. Thus, within experimental error, there are four Cd(A), four Cd(B), and two Cd(C) sites in the decanuclear cation. High-resolution magnifications of the A and C resonances, shown in Figure 2, indicate that these bands are further split by 3.0 and 5.4 ± 0.5 ppm, respectively. Since our spectra are proton decoupled, no $^{113}Cd-^{1}H$ J coupling is observed and at 12.34% natural abundance the probability of adjacent $^{113}Cd-^{113}Cd$ J coupling is too small to affect our line widths.

The components of the shielding tensors have been measured by the combination of OMAS and static spectrum synthesis described above. The anisotropic shieldings of each of the A and C bands were approximated by single anisotropic shielding tensors. We feel this simplification to be valid since the static spectrum is well fitted by three powder patterns of shielding tensors. Furthermore, relative areas and isotropic shifts are in complete accord with the MAS data. All measurements indicate that the shielding tensor of A is axially symmetric while those of B and C are nonaxially symmetric. B has the largest anisotropy, or line width, which is about twice as large as those of A and C. Rotation factors, R, defined by eq 16, were calculated for each tensor and are listed in Table I also. While our rotor speed, ω_r = 2.9 kHz, is sufficient to satisfy the inequality (15) for the A and C anisotropies, such a speed is far below the ca. 5 kHz required to satisfy (15) for the B anisotropy. Consequently, large asymmetric spinning satellites (labeled SS_B) occur in the MAS spectrum shown in Figure 1 and in the OMAS spectrum (spinning satellites not shown).[18]

As described above, the static spectrum shown in Figure 3 was synthesized by a nonlinear least-squares line-shape fitting analysis with the inferred estimates of the shielding components from the OMAS measurements serving as "initial guesses". OMAS values, in terms of $\bar{\sigma}$, $\Delta\sigma'$, and S are listed in Table II; static values are given in Table I. We note that for this particular molecule static and MAS data are sufficient to determine the 8 σ_i (three each for B and C, two for A) from 11 known values: the 8 maxima in the static spectrum plus the 3 $\bar{\sigma}$ from the MAS spectrum. The accuracies of these values may be inferred by comparing the static isotropic values and area ratios to those of the MAS spectrum.

Our solid samples of $Cd(ClO_4)_2 \cdot 6H_2O$, CdO, and CdS gave resonances at −105 ± 5, −515 ± 10, and −808 ± 5 ppm, respectively. Aqueous solutions of $Cd(ClO_4)_2$(2, 1, and 0.5 M) gave single resonances at 121 ± 5 ppm. We find in agreement with previous workers[1,2] that the chemical shift of $Cd(ClO_4)_2$ in water is nearly independent of concentration.

Crystals of $[Cd_{10}(SCH_2CH_2OH)_{16}](ClO_4)_4$ are monoclinic with unit cell parameters closely resembling those published for the sulfate salt.[13]

Discussion

The X-ray determination of the structure of the sulfate salt of $Cd_{10}(SCH_2CH_2OH)_{16}^{4+}$ has been reported.[13,14,18] The Cd–S framework is shown in Figure 1. Cadmium atoms 5 and 6 located on the crystallographic C_2 axis have a distorted tetrahedral CdS_4 coordination sphere ($Cd-S_{av}$ = 2.51 Å). Cadmium atoms 7–10 have a trigonal-bipyramidal CdS_4O coordination with the O in one of the axial positions ($Cd-S_{eq}$ = 2.52 Å, $Cd-S_{ax}$ = 2.86 Å, $Cd-O_{ax}$ = 2.41 Å). Finally cadmium atoms 1–4 have a distorted *fac*-octahedral coordination of CdS_3O_3 ($Cd-S_{av}$ = 2.56 Å, $Cd-O_{av}$ = 2.46 Å). Except for the long axial bond, Cd–S distances are normal compared with those of other structures, in particular with that of CdS, which is about 2.53 Å.[19] The Cd–O distances are also similar to that of CdO which is about 2.35 Å.[19]

The above structural data may be correlated with our NMR data as follows. (1) From the area ratios, we assign the C band to the CdS_4 sites. Each Cd^{2+} in CdS has a tetrahedral CdS_4 coordination sphere similar to that of the CdS_4 in the decanuclear complex. Since Cd–S distances are more or less the same for both materials, it is no surprise to find that the isotropic shift of ^{113}Cd in CdS at −808 ppm is close to that of the C band at −773 ppm. (2) We assign the A band to the CdS_3O_3 sites and the intermediate B band to the CdS_4O sites. These assignments are consistent with those made by Haberkorn et al.[2] for the ^{113}Cd NMR spectrum of a solution of this ion. The relatively large anisotropy of the B band supports its assignment to the CdS_4O sites because there is a larger difference in bond distances between $Cd-S_{eq}$ and $Cd-S_{ax}$ than between $Cd-S_{av}$ in either the CdS_4 or CdS_3O_3 sites. The shielding symmetry factor, S = 0.72, of the B band assigned to the CdS_4O sites is very high although somewhat less than the axially symmetric factor, S = 1, of the A band assigned to the CdS_3O_3 sites.

The isotropic shift assigned to the CdS_3O_3 site (−509 ppm) is at about the same location as that of CdO (−515 ppm). CdO crystallizes in a cubic structure with NaCl arrangement. Each

(18) Our preliminary results indicate an even larger B anisotropy for the sulfate salt of the decanuclear cation which leads to increases in the intensities of the spinning satellites and complicates the spectral analysis. We also note a significantly larger splitting of the C resonance. The locations of the sulfate anions in the crystal have apparently not been published.

(19) Wykoff, R. W. G. "Crystal Structures", Wiley: New York, 1965; Vol. 1.

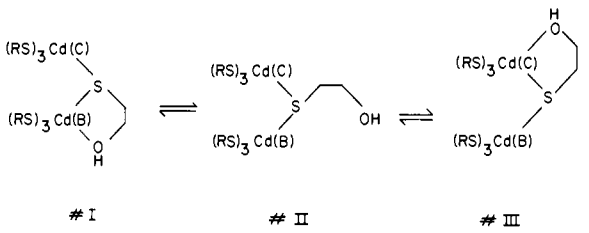

Figure 4. Postulated mechanism for B ⇄ C site exchange in $[Cd_{10}(SCH_2CH_2OH)_{16}](ClO_4)_4$ (adapted from ref 2).

Cd has an octahedral CdO_6 coordination.[19] Combining these observations with our measurement of the CdS chemical shift leads to an interpretation that increasing the numbers of either oxygens or sulfurs of sp^3 valence orbital hybridization around Cd^{2+} increases the shielding of the ^{113}Cd nucleus. Viewed in this light, one can interpret the observed B anisotropy by considering the CdS_4O sites to be nearly axially symmetric and approximating the B tensors as $\sigma_{\parallel}^B = \sigma_{11}^B$ and $\sigma_{\perp}^B = (\sigma_{22}^B + \sigma_{33}^B)/2$. If one assumes the S_{ax}---Cd–O_{ax} to be the local unique axis, $\sigma_{\parallel}^B$, then one expects the Cd^{2+} to be more shielded in the perpendicular, degenerate directions $\sigma_{\perp}^B$, which are in the plane of the three equatorial sulfur atoms, than along $\sigma_{\parallel}^B$ whose axis contains only one oxygen atom and one distant sulfur atom. Thus, the $\sigma_{\perp}^B$ shielding component should occur upfield from the $\sigma_{\parallel}^B$ shielding component—as is observed. The removal of the degeneracy of $\sigma_{\perp}^B$ may arise from one of the equatorial sulfurs bridging three cadmiums whereas the others bridge only two cadmiums.

We also note that the CdS_3O_3 sites appear to have the local threefold axis required for the observed axially symmetric tensor. However, crystals of the $[Cd_{10}(SCH_2CH_2OH)_{16}](ClO_4)_4$ are monoclinic and C_2 is the highest symmetry axis allowed in this crystal system. Thus, the values of the symmetry factor for both the A and B shielding anisotropies reflect approximate local rather than crystallographic symmetries.

Haberkorn et al.[2] interpreted their solution NMR data by assuming that the decanuclear cation has S_4 symmetry, meaning that all cadmium sites with the same coordination sphere are equivalent and should give rise to a single resonance. Our MAS spectrum indicates that, despite the crystallographic restriction on symmetry axes, for NMR purposes the local environment of the cation in the solid also closely approximates S_4 symmetry since only three major resonances are obtained, one for each coordination sphere. The small additional splittings of the A and C resonances, however, indicate that strict S_4 symmetry is not observed. Without knowing the locations of the perchlorate anions and other details of the crystalline environment of the decanuclear cation, we refrain from interpreting these small splittings on a molecular basis.[18]

Haberkorn et al.[2] observed only two resonances in the ^{113}Cd NMR spectrum of $[Cd_{10}(SCH_2CH_2OH)_{16}](ClO_4)_4$ in dimethylformamide (DMF) between −40 and 60 °C. The two resonances are separated by 133 ppm at 20 °C and 150 ppm at −20 °C. The downfield resonance is considerably broadened at −40 °C. They concluded that the upfield resonance is due to the CdS_3O_3 sites, whereas the downfield resonance is the change-averaged band resulting from interconversion of the CdS_4 and CdS_4O environements. A possible mechanism for this interconversion is shown in Figure 4.[2]

Obviously site interconversion does not occur in solid $[Cd_{10}(SCH_2CH_2OH)_{16}](ClO_4)_4$ since three resonances are obtained. In order to compare the solution results with ours, we approximate the resonance for the fast exchange between CdS_4 and CdS_4O as the weighted average of the C and B bands, i.e., $-(2 \times 773 + 4 \times 602)/6 = -659$ ppm. The separation of this calculated exchange resonance from band A (the CdS_3O_3 site) is then found to be 150 ppm, in good agreement with the solution spectra between 20 and −40 °C.[2] This analysis assumes that the intermediate (II of Figure 4) has a short lifetime compared with those of the final states (I and III of Figure 4). Moreover, our solid-state spectra yield additional information about the exchange process. Assuming that the 171 ppm (~2.1 kHz) separation between resonances C and B represents the slow exchange limit between CdS_4 and CdS_4O sites, then using the coalescence criterion for two-site exchange, $\Delta\nu = k_e/2\pi$ as a crude approximation, the exchange rate, k_e, between CdS_4 and CdS_4O sites in DMF solution must be faster than about 1.3×10^4/s above −40 °C.

Since spectra of rare spins in solution cannot be obtained under conditions identical with those used for high-resolution spectra of solids, we have not measured the chemical shifts of solids with respect to the usual solution reference, 0.1 M $Cd(ClO_4)_2$.[1-5] We have chosen solid $Cd(NO_3)_2 \cdot 4H_2O$ as a reference in the past[9,11] because it gives the most shielded chemical shift of all the easily obtainable cadmium salts. However, based on our data for aqueous $Cd(ClO_4)_2$, the following conversion can be made:

$$\delta = -\bar{\sigma} - 121\ (\pm 5\ \text{ppm}) \qquad (19)$$

where δ and $\bar{\sigma}$ are in ppm relative to 0.1 M $Cd(ClO_4)_2$ and solid $Cd(NO_3)_2 \cdot 4H_2O$, respectively. The ±5-ppm uncertainty is due mainly to differences in bulk susceptibilities between the various solutions and solid samples. Application of (19) to our MAS spectrum of solid $[Cd_{10}(SCH_2CH_2OH)_{16}](ClO_4)_4$ results in calculated δ values of 388, 481, and 652 ppm for bands A, B, and C, respectively. The calculated position of the A band on the δ scale falls within the range of 400–378 ppm measured by Haberkorn et al.[2] for the same band in DMF solution between +40 and −40 °C. The calculated position of the C band falls within the range of 670–604 ppm observed for ^{113}Cd resonances of metallothionen.[4] Compared to our results this range indicates that the ^{113}Cd resonances observed for metallothionen are not due to CdS_4O and CdS_3O_3 environments and is consistent with the CdS_4 coordination sphere proposed for all cadmiums in metallothionen by Otvos and Armitage.[4b,20]

Conclusions

In light of the above discussion, we can summarize the general correlations of each of the three shielding parameters $\bar{\sigma}$, $\Delta\sigma$, and S to certain structural aspects as follows. (1) The isotropic shift, $\bar{\sigma}$, measures the average shift at a given nucleus and thus indicates the kinds of nearest neighbors in much the same manner as the lines of a solution NMR spectrum, but without the complicaton of exchange averaging. The crystallographic point symmetry seems to have only a small effect on $\bar{\sigma}$ since we detect only small splittings of the A and C bands and no splitting of the B band. (2) The shielding anisotropies, $\Delta\sigma$, measure the three-dimensional variations in shieldings and thus indicate the range of bonding distances of nearest neighbors. For example, the CdS_4O site which contains large variations in bonding distances in a pesudo-axial direction (discussed above) has a relatively large anisotropy, whereas the CdS_4 site which is pseudo-tetrahedral with relatively uniform bonding distances has a much smaller anisotropy. Finally, (3) the symmetry factor, S, measures the uniformity of shielding with respect to an axially symmetric tensor in which shielding in two of the three principal directions are equivalent. For example, while the CdS_4O site has a relatively large anisotropy, it nevertheless has a relatively high symmetry factor which suggests that the shielding is close to being axially symmetric. In contrast, the "pseudo-tetrahedral" CdS_4 site which has the smallest anisotropy has the lowest symmetry factor, implying that shieldings are quite different in the three principal directions.

We have also demonstrated that our techniques are useful for interpreting exchange phenomena observed by NMR in solution. Our chemical shifts for the decanuclear cation, converted to a 0.1 M $Cd(ClO_4)_2$ reference agree quite well with those obtained in solution and suggest CdS_4 ligation for the ^{113}Cd resonances observed in metallothionen.

We think that our results fulfill possibilities 1 and 2 stated in the Introduction and, coupled with solution data, demonstrate the feasibility of using high-resolution ^{113}Cd NMR of solids to obtain

(20) If our interpretation that sp^3 oxygens and sulfurs provide about equal shielding is correct, then it is possible that the ^{113}Cd resonances observed for metallothionen are due to CdS_3O, CdS_2O_2, $CdSO_3$, or CdO_4 sites as well as CdS_4 sites.

(21) Bloembergen, N.; Rowland, J. A. *Acta Metall.* **1953**, *1*, 731–736.

useful structural and dynamic information about Cd^{2+} in large molecules.

Acknowledgment. D.M.K. acknowledges support from donors of the Petroleum Research Fund, administered by the American Chemical Society. S.L. acknowledges support by a "Postgraduate Scholarship" from the Natural Sciences and Engineering Research Council of Canada. We thank Dr. Bruce Parkinson for donating the sample of CdS and James Richardson for determining the unit cell parameters of $[Cd_{10}(SCH_2CH_2OH)_{16}](ClO_4)_4$. The Ames Laboratory is operated for the U.S. Department of Energy by Iowa State University under Contract No. W-7405-Eng-82. This research was supported by the Assistant Secretary for Energy Research, Office of Energy Sciences, WPAS-KC-03-02-01.

Analysis of Field-Dependent Relaxation Data and Hyperfine Shifts of Cytochrome *c'* from *Rhodospirillum rubrum* in Terms of the High-Spin Iron Ligation States

Gerd N. La Mar,* J. Timothy Jackson, and R. G. Bartsch†

Contribution from the Departments of Chemistry, University of California, Davis, California, 95616, and University of California, San Diego, La Jolla, California 92093.
Received December 18, 1980

Abstract: The pH and field dependence of the paramagnetic line widths of the heme methyl resonances of cytochrome *c'* from *Rhodospirillum rubrum* (strain 1 DTCC) have been analyzed for the purpose of extracting information on the ligation states of the protein in both its oxidized and its reduced high spin forms. The methyl line widths in all protein forms were found to exhibit substantial quadratic field dependence consistent with significant contribution from Curie spin relaxation. For ferricytochrome *c'*, the field-independent contribution to the methyl line width differed substantially between the acid-to-neutral pH form (I) and form II, stable in the pH range 9–11. Comparison of the calculated electron relaxation times indicates that form I has a weaker axial ligand field than either form II or aquometmyoglobin, which favors a five-coordinate I and a six-coordinate II. The appearance of two new resonances in the far downfield region upon converting I → II, without the apparent loss of any hyperfine shifted signals from I, confirms the coordination of a sixth ligand in II. Qualitative comparisons of the line widths of these two new signals to those of the heme methyls support an acidic residue as the sixth ligand. The detection of the characteristic exchangeable proton resonance of an axial imidazole and the importance of Curie spin relaxation in ferrocytochrome *c'* confirm its high-spin five-coordinated structure.

Cytochromes *c'* are a group of primarily dimeric hemoproteins found in a variety of photosynthetic and denitrifying bacteria. Although their precise function remains to be established, cytochromes *c'* probably act as electron-transport proteins.[1] Initial spectroscopic[2,3] and susceptibility[4,5] studies revealed these proteins to be essentially high spin in both their redox states, in contrast to the more usual low-spin mitochondrial or bacterial cytochromes *c*. They share with the latter class of proteins[6] the invariant peptide fragment, Cys-X-X-Cys-His (Figure 1A), toward the C-terminal end of the molecules at residues approximately 116–120. While this fragment provides both the covalent links to the heme and the axial histidyl imidazole[7,8] the nature of the sixth ligand, at least in the ferric state, remains in question in all three of the forms the protein adopts in different pH ranges. A single-crystal X-ray diffraction study[9] of the dimeric cytochrome *c'* from *Rhodospirillum molischianum* has confirmed an axial histidine for each of the equivalent ferric hemes, but the resolution is not yet sufficiently high to permit unambiguous conclusions as to the presence of a coordinated water in the neutral pH form of the protein.

For the ferrous form in the neutral pH range, optical, susceptibility, near-infrared MCD, and resonance Raman data all agree on a five-coordinated form very similar to deoxymyoglobin.[2-5,10-13] The ferric form adopts three spectroscopically distinct forms designated I (pH 5–9), II (pH 9–11), and III (pH ≥12).[2] Early ESR[10] and resonance Raman[11] work revised the original high-spin formulation for I at low pH, instead suggesting the existence of a quantum mechanical mixed-spin, $S=^3/_2, ^5/_2$, state. More recent Mössbauer[12] and near-IR MCD[13] data, however, favor the initial high-spin ground state. Although resonance Raman spectra were originally interpreted[14] in terms of a five-coordinate species for I, subsequent revision has suggested[15] a six-coordinate species with an oxygen-bound ligand that is lost upon converting to II in the weakly alkaline region. In contrast, the increase in energy of near-IR bands on converting from I → II has led to the proposal that a five-coordinate species

† University of California, San Diego.

(1) Bartsch, R. G. In "The Photosynthetic Bacteria"; Clayton, R. K., Sistrom, W. R., Eds.; Plenum Press: New York, 1978; 249–279.
(2) Horio, T.; Kamen, M. D. *Biochim. Biophys. Acta* **1961**, *48*, 266–286. Imai, Y.; Imai, K.; Sato, R.; Horio, T. *J. Biochem (Tokyo)* **1969**, *65*, 225–237. Kamen, M. D.; Kakuno, T.; Bartsch, R. G.; Hannon, S. *Proc. Nat. Acad. Sci. U.S.A.* **1973**, *70* 1851–1854.
(3) Moss, T. H.; Bearden, A. J.; Bartsch, R. G.; Cusanovich, M. A. *Biochemistry* **1968**, *7*, 1583–1590.
(4) Ehrenberg, A.; Kamen, M. D. *Biochim. Biophys. Acta* **1965**, *102*, 333–340.
(5) Tasaki, A.; Otsuka, J.; Kotani, M. *Biochim. Biophys. Acta* **1967**, *140*, 284–290.
(6) Salemme, F. R. *Annu. Rev. Biochem.* **1977**, *46*, 299–329.
(7) Meyer, T. E.; Ambler, R. P.; Bartsch, R. G.; Kamen, M. D. *J. Biol. Chem.* **1975**, *250*, 8416–8421.
(8) Ambler, R. P.; Daniel, M.; Meyer, T. E.; Bartsch, R. G.; Kamen, M. D. *Biochem. J.* **1979**, *177*, 819–823.
(9) Weber, P. C.; Bartsch, R. G.; Cusanovich, M. A.; Hamlin, R. C.; Howard, A.; Jordan, S. R.; Kamen, M. D.; Meyer, T. E.; Weatherford, D. W.; Xuong, Ng. H.; Salemme, F. R. *Nature (London)* **1980**, *286*, 302–304.
(10) Maltempo, M. M.; Moss, T. H.; Cusanovich, M. A. *Biochim. Biophys. Acta* **1974**, *342*, 290–305.
(11) Strekas, T. C.; Spiro, T. G. *Biochim. Biophys. Acta* **1974**, *351*, 237–245.
(12) Emptage, M. H.; Zimmermann, R.; Que, Jr., L.; Münck, E.; Hamilton, W. D.; Orme-Johnson, W. H. *Biochim. Biophys. Acta* **1977**, *495*, 12–23.
(13) Rawlings, J.; Stephens, P. J.; Jafie, L. A.; Kamen, M. D. *Biochemistry* **1977**, *16*, 1725–1729.
(14) Kitagawa, T.; Ozaki, Y.; Kyogoku, Y.; Horio, T. *Biochim. Biophys. Acta* **1977**, *493*, 1–11.
(15) Teraoka, J.; Kitagawa, T. *J. Phys. Chem.* **1980**, *84*, 1928–1935.

0002-7863/81/1503-4405$01.25/0